

Cooperative Segmental Motions in Ethyl Acrylate/Triethylene Glycol Dimethacrylate Copolymer Networks Studied by Dielectric Techniques

Andreas T. Stathopoulos,^{*,†} Apostolos Kyritsis,[†] Gloria Gallego Ferrer,^{‡,§,⊥} José Luis Gómez Ribelles,^{‡,§,⊥} Costas Christodoulides,[†] and Polycarpos Pissis[†]

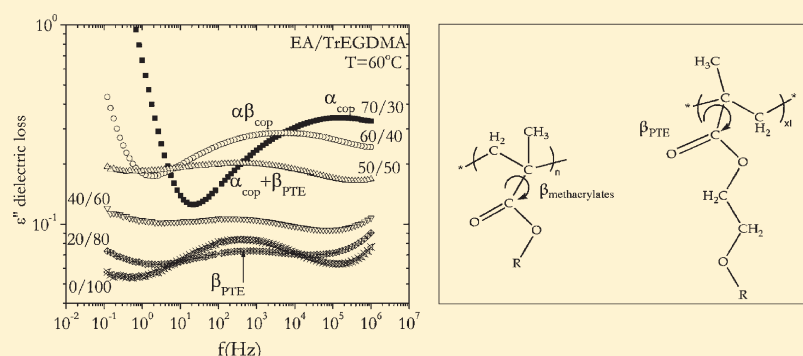
[†]Department of Physics, National Technical University of Athens, Zografou Campus, 15780 Athens, Greece

[‡]Centro de Biomateriales e Ingeniería Tisular, Universidad Politécnica de Valencia, P.O. Box 22012, E-46071 Valencia, Spain

[§]Regenerative Medicine Unit, Centro de Investigación Príncipe Felipe, Autopista del Saler 16, 46013 Valencia, Spain

[⊥]CIBER en Bioingeniería, Biomateriales y Nanomedicina, Valencia, Spain

ABSTRACT:



The molecular dynamics of ethyl acrylate/triethylene glycol dimethacrylate (EA/TrEGDMA) copolymer networks on the overall composition range were investigated thoroughly by employing dielectric techniques: thermally stimulated depolarization currents (TSDC) and dielectric relaxation spectroscopy (DRS). Furthermore, differential scanning calorimetry (DSC) was performed in order to investigate the thermal glass transition of these copolymers. The results show that, for low content of the TrEGDMA component, the overall dielectric behavior of the copolymers is dictated by the dynamics of PEA component, exhibiting the α_{cop} relaxation process which is strongly affected by the TrEGDMA moieties becoming broader and shifting to higher temperatures with increasing cross-linker (TrEGDMA) content. For the copolymer networks rich in TrEGDMA ($w_{\text{TE}} \geq 40$ wt %), the overall dielectric behavior indicates that the dynamics of the dimethacrylate component dominates, resembling that of poly(*n*-alkyl methacrylates) in the sense that the temperature dependence of molecular relaxation processes presents a merging region where the local relaxation process of TrEGDMA, β_{PTE} , merges with the more cooperative α_{cop} process of the copolymers into an $\alpha\beta_{\text{cop}}$ locally cooperative relaxation process. By increasing the EA content, the strength of α_{cop} relaxation process enhances and simultaneously the merging region shifts to lower temperatures. The cooperative motions are significantly suppressed in the copolymers with TrEGDMA contents higher than 80 wt %. The copolymers present enhanced spatial heterogeneity the more TrEGDMA content, whereas no dynamic heterogeneity was detected.

INTRODUCTION

Polymer networks have attracted much interest in material science both for technological and physical reasons. From the technological point of view, hydrophilic polymer networks have been tailored as appropriate systems to be useful in the form of hydrogels for biological applications, i.e., tissue scaffolds, drug delivery systems.^{1,2} Furthermore, polymer networks are used as suitable systems for coating, optoelectronic applications, and biological applications (dental materials).^{3–6} In order to improve their properties toward desirable directions, it is essential to understand the structure–property relationship of these systems.

The investigation of molecular dynamics in polymer networks by varying the cross-linking density is a methodology widely used by many researchers in order to extract information on the structure of these systems.^{7–13}

The hardening of a simple polymer in order to comprise a polymer network is achieved by using a hardener (cross-link agent). The addition of a hardener forms chemical cross-link junctions

Received: July 29, 2011

Revised: September 12, 2011

Published: September 29, 2011

among polymer chains and induces with this manner spatial restrictions leading to the increase of the respective glass transition and affecting the final properties of the segmental relaxation process.^{7,9,11,14–18} A lot of interest has been paid in the investigation of the critical length between cross-linked junctions for which the temperature dependence of relaxation times changes under the controlled buildup of cross-linking network.^{13,19,20} However, the buildup of cross-linking density is not always well controlled, and several factors as the structure and the reactivity of the respective monomer and that of cross-linker agent have to be taken into consideration.^{21–23} It is well established that the increase of cross-linking density is usually accompanied by the broadening of glass transition region even for low contents of hardener, an effect which is attributed to the existence of nano-domains with different mobilities.^{9–12} The heterogeneity in cross-linking density distribution is the reason from this broadening and has been detected through static and dynamic light scattering experiments^{24–26} as well as by structural relaxation experiments.¹⁵ Furthermore, the inherent heterogeneities and the presence of cross-link agglomerations in polymer networks have also been predicted by theoretical approaches.²⁷ In this context, it is interesting the investigation of the glass transition and cooperative dynamics in polymer/hardener systems extended to the whole composition range, namely from the linear polymer toward the highly dense network of the multifunctional cross-linker.¹¹

The present system is consisted of a simple monofunctional monomer ethyl acrylate (EA), which, under radical polymerization, forms the well-known poly(ethyl acrylate) (PEA). PEA was reticulated by using the multifunctional component triethylene glycol dimethacrylate (TrEGDMA). TrEGDMA is well-known as basic material used in electro-optical devices, spherical lenses, coating, and dental material,^{6,28,29} either as an individual component or in the form of copolymer with other dimethacrylates.^{30,31} It is well established in the literature that the family of dimethacrylates (TrEGDMA included), after radical polymerization, create heterogeneous structures characterized by the presence of highly cross-linked regions called microgels. Microgels comprise densely cross-linked and cycled domains which are formed during the first stages of radical polymerization nearby the sites of the initial radicals.^{21,22,32–35} Cyclization is a significant factor for their formation and is more pronounced the lower the length of the reacted dimethacrylate^{36,37} and the higher the functionality of the reacted dimethacrylate monomers.³⁸ During the evolution of radical polymerization, the microgels develop agglomerates. Their size varies between 10 and 400 nm according to light scattering measurements in similar systems performed by Rey and co-workers.²¹ Evidence of the existence of loosely cross-linked regions around microgels during radical polymerization has been found in similar systems.^{21,22,33,39}

The dielectric characteristics of dense net-TrEGDMA are of high interest, mainly due to the fact that the high cross-linked network results to the entire depression of segmental dynamics.⁴⁰ Viciosa and co-workers observed dielectrically this depression by monitoring the dielectric relaxations of triethylene glycol,⁴⁰ tetraethylene glycol dimethacrylate (TEGDMA), and diethylene glycol dimethacrylate (DiEGDMA) from monomer to net-TEGDMA and net-DiEGDMA, respectively.⁴¹ Interestingly, these studies revealed that the β_{PTE} relaxation process in dimethacrylates (secondary process emerged after the polymerization) possesses the same position with β process of poly(methyl methacrylate) in the corresponding Arrhenius plots.⁴¹

In the present work a soft component, ethyl acrylate (EA), is reacted with TrEGDMA moieties forming the copolymer networks EA/TrEGDMA. The aim of the present work is to investigate the effect of the one component to the dynamics of the other by means of the study of molecular dynamics in the overall composition range of EA/TrEGDMA copolymer series. The addition of a soft component (here EA) is expected to facilitate cooperative segmental motion in a highly dense network. Interesting enough is the determination of the critical composition, for which the copolymer changes its dynamical characteristics dictated by the one component to that dictated by the other. Aiming at these goals, the photopolymerized EA/TrEGDMA copolymer networks expanding the whole composition range, namely from 100/0 to 0/100, were investigated by employing the dielectric techniques of thermally stimulated depolarization currents and dielectric relaxation spectroscopy. The glass transition was studied by differential scanning calorimetry.

■ EXPERIMENTAL SECTION

Monomers of ethyl acrylate (EA) and triethylene glycol dimethacrylate (TrEGDMA) supported by Aldrich were used without purification. A mixture by changing the components composition with a step 10 wt % was prepared. The polymerization of the components mixture was performed with 0.15 wt % of benzoin under ultraviolet light for ~ 18 h to ensure full conversion. Plate sheets with a width around 0.5 mm were prepared. The samples were purified in boiled ethanol for 24 h in order to remove low molecular weight residuals produced during polymerization. Then the samples were dried in vacuum for 48 h at temperatures ranging from 60 to 200 °C (above the respective glass transition) so as to remove ethanol residuals. The codification of the produced copolymer networks EA/TrEGDMA has the form EA/TrEGDMA, where EA and TrEGDMA are the weight fractions of respectively ethyl acrylate and triethylene glycol dimethacrylate; for instance, the codification 60/40 represents the copolymer network with 60 wt % EA and 40 wt % TrEGDMA. The subscripts used in the text are as follows: “cop” is referred to the copolymer, “TE” stands for processes detected in TrEGDMA unreacted groups, “PTE” stands for processes detected only in polymerized TrEGDMA, and “PEA” corresponds to processes produced from PEA.

Differential scanning calorimetry (DSC) was performed in a Mettler Toledo DSC 823E apparatus. The samples were subjected to a cooling scan from ambient temperature down to -70 °C, followed by a heating scan from that temperature up to 180 °C (except for homopolymer PEA, where the temperature range spanning -100 to 50 °C), both scans with a rate of 10 K/min. In the meantime of cooling and heating scans the samples remain at the lowest temperature for 5 min in order to equilibrate. Nitrogen gas was let through the DSC cell with a flow rate of 30 mL/min. Temperature was calibrated with indium and zinc standards. The melting heat of indium was used for calibrating the heat flow. The samples were packed in aluminum pans.

TSDC measurements were performed on copolymer networks EA/TrEGDMA, in the temperature interval between -150 and 180 °C under nitrogen flow, controlled by a Novocontrol Quatro Cryosystem. In TSDC experiment, the sample is inserted between the brass plates of a capacitor and polarized by the application of electric field E_p at a temperature T_p (temperature of polarization) for time t_p . With the electric field still applied, the sample is cooled to temperature T_0 (which was sufficiently low to prevent depolarization by thermal excitation) and then is short-circuited and reheated at a constant rate b . In our experiments the resulting discharge current was measured as a function of temperature by means of a Keithley 617 electrometer with an accuracy of 0.01 pA. The equivalent frequency f of TSDC measurements spans $10^{-4} < f < 10^{-2}$ Hz; i.e., it is close to those of DSC measurements.⁴²

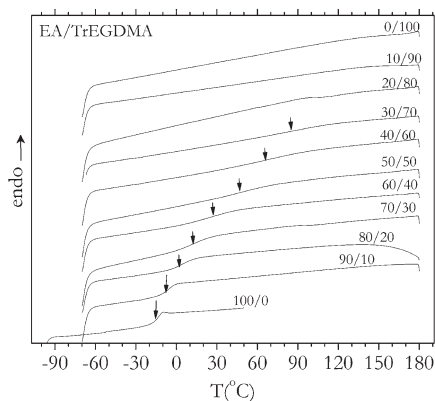


Figure 1. DSC heating scans corresponding to EA/TrEGDMA copolymer networks for variant compositions, including the neat PEA and net-TrEGDMA homopolymers. The arrows indicate the estimated glass transition temperature.

TSDC is characterized by high sensitivity, which allows the detection of weak relaxations.⁴³ Typical experimental conditions for the ordinary TSDC measurements were $E_p = 1\text{--}5$ kV/cm for the polarizing field, $t_p = 5$ min for the polarization time, 10 K/min for the cooling rate to $T_0 = -150$ °C, and $b = 3$ K/min for the heating rate. The polarization temperature (T_p) was selected at temperatures above the respective glass transition of the measured copolymer networks, ranging from 0 to 80 °C. For the samples 20/80, 10/90, and 0/100, the polarization temperature was selected at 140, 150, and 180 °C, respectively.

DRS measurements were performed with an Alpha analyzer combined with a Quatro temperature control system, both supported by Novocontrol. The complex dielectric permittivity $\epsilon^*(f) = \epsilon'(f) - i\epsilon''(f)$ was obtained isothermally in steps of 5 deg in the temperature interval from -150 to 180 °C. The frequency window for the isothermal measurements was determined in a range from 10^{-1} to 10^6 Hz. A detailed description of the method may be found elsewhere.⁴⁴

RESULTS

Differential Scanning Calorimetry (DSC). The DSC thermograms were carried out covering a temperature range from -70 to 180 °C (except for homopolymer PEA: -100 to 50 °C), with cooling and heating rates at 10 K/min. Figure 1 portrays the respective heating thermograms corresponding to EA/TrEGDMA copolymer networks for variant compositions. The recorded thermograms show only one glass transition temperature, which shifts toward higher temperatures with increasing TrEGDMA content. For TrEGDMA contents above 70 wt %, the respective glass transition endothermic step in the thermograms is not detectable. Noteworthy is the significant broadening of glass transition temperature range ($\Delta T = T_{\text{end}} - T_{\text{onset}}$) that exceeds 40 °C, for TrEGDMA contents above 40 wt % (Table 1). Interesting enough is also the systematic decrease of heat capacity increment with the addition of TrEGDMA (Table 1). However, it is worth noticing that for TrEGDMA contents higher than 50 wt % the estimation of the heat capacity increment contains significant uncertainty due to the tremendous broadening of the glass transition region. In any case, the decrease of the heat capacity step with increasing TrEGDMA content is beyond the experimental uncertainty, implying the decrease of the available configurations for the copolymer motions during the glass transition with the addition of cross-linker.

Table 1. Copolymer Network Glass Transition Temperature, Heat Capacity Increment, and Glass Transition Temperature Interval for Several TrEGDMA Contents As Estimated by DSC Heating Scans

EA/TrEGDMA	T_g (°C)	ΔC_p (J/(g °C))	ΔT (°C)
100/0	-15 ± 1	0.400 ± 0.002	8 ± 1
90/10	-7 ± 1	0.395 ± 0.002	11 ± 1
80/20	3 ± 2	0.357 ± 0.002	16 ± 2
70/30	12 ± 2	0.344 ± 0.003	23 ± 2
60/40	27 ± 3	0.322 ± 0.008	40 ± 3
50/50	50 ± 4	0.25 ± 0.02	51 ± 5
40/60	70 ± 6	0.29 ± 0.04	71 ± 8
30/70	85 ± 15	0.20 ± 0.06	72 ± 12

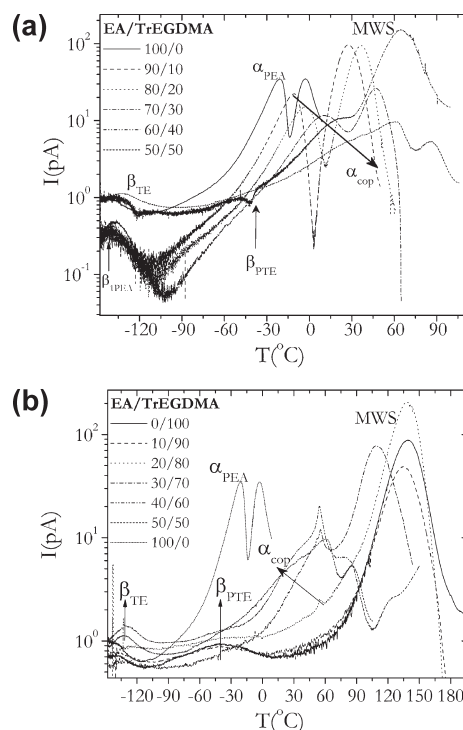


Figure 2. TSDC thermograms (transient depolarization current against temperature) regarding the EA/TrEGDMA copolymer networks for the overall TrEGDMA content range. (a) TrEGDMA contents from 0 to 50 and (b) 50 to 100 (including neat PEA).

Thermally Stimulated Depolarization Currents (TSDC). The global TSDC thermograms were recorded with a heating rate 3 K/min covering a temperature range from -150 to 180 °C (for the homopolymer PEA the measured temperature range was -150 to 30 °C). The polarization temperature (T_p) was selected at temperatures above the respective glass transition of the measured copolymer networks, ranging from 0 to 80 °C. For the samples 20/80, 10/90, and 0/100, for which no glass transition temperature was detected by DSC measurements, the polarization temperature was selected at 140, 150, and 180 °C, respectively.

The α_{PEA} relaxation process, related with segmental mobility of polymer chains regarding the linear PEA, is depicted in Figure 2a accompanied by a second peak at -3 °C, both well

discerned. Because of the absence of chemical cross-links in homopolymer PEA, it is an open question whether the second peak is a Maxwell–Wagner–Sillars (MWS) peak or a ρ -peak.⁴³ By increasing TrEGDMA content, the system becomes a random copolymer network. Thereby, the primary dipolar peak is ascribed to copolymer segmental motions, so denoted as α_{cop} . The primary dipolar peak (α_{cop}) is accompanied by a second peak (MWS) which is derived from the trapped charges into interfaces induced by the heterogeneities from the random cross-linking. The addition of TrEGDMA broadens α_{cop} process and shifts it toward higher temperatures, in parallel to the shift of the MWS peak which remains well separated from the dipolar α_{cop} peak. However, for 40 wt % TrEGDMA some significant changes in TSDC thermograms occur. The α_{cop} relaxation is now not well discerned being overlapped with the MWS peak and appears as a shoulder at the low-temperature side of the MWS peak. Despite our experimental efforts to separate the two contributions by decreasing the polarization temperature (T_p), we were not able to separate the dipolar segmental polarization from the MWS polarization although the intensity of the later peak was remarkably reduced (results not shown here). Similar features exhibit the thermograms obtained on the samples 50/50, 40/60, and 30/70 and are shown in Figure 2b. Noteworthy is the presence of a sharp peak at 54 °C for the samples 40/60 and 30/70 that appears systematically, even with no field excitation. The origin of this current release is not clear yet. Another significant feature is the emergence of the secondary relaxation process β_{PTE} , which is well discerned for high contents of TrEGDMA (Figure 2b), and its contribution can be observed already for the sample 60/40 as an increase in the transient current background in the temperature range between –100 and 0 °C (Figure 2a, a dispersion not present in TSDC thermograms on copolymer networks 90/10, 80/20, and 70/30). Also, it is worth mentioning the presence of β_{TE} process in the same TrEGDMA content range at approximately –130 °C. The origin of these secondary dipolar processes is related to TrEGDMA local motions and will be discussed later in the section devoted to DRS results. The appearance of these low-temperature peaks and the significant overlapping between α_{cop} and MWS peak for TrEGDMA contents higher than 30% signifies the change in the molecular dynamics of EA/TrEGDMA copolymer networks at this TrEGDMA content region. Finally, it is interesting to point out that the high-temperature side of the TSDC thermograms obtained on the copolymer networks for high TrEGDMA contents (20/80, 10/90, and 0/100) presents only one large peak at 135–140 °C. The position of this peak is the same for these samples, while for the copolymer network 20/80 a small shoulder at the low-temperature side is clearly observed. Presumably this large peak is the respective MWS peak, while the small shoulder is the respective α_{cop} process.

Dielectric Relaxation Spectroscopy (DRS). Broadband dielectric relaxation spectroscopy was employed for EA/TrEGDMA copolymer networks in a frequency window spanning 10^{-1} to 10^6 Hz in a temperature range from –150 to 180 °C. The isochronal plots of the imaginary part of dielectric permittivity against temperature, extracted by the data recorded isothermally, were constructed so as to present the relaxation processes existed in the copolymers under study in a form comparable to the aforementioned TSDC thermograms. The isochronal plots of ϵ'' at 1 kHz (Figure 3) were selected in order to avoid conductivity effects at high temperatures that mask the primary dielectric relaxations as previously observed in TSDC measurements (equivalent frequency at 1 mHz).

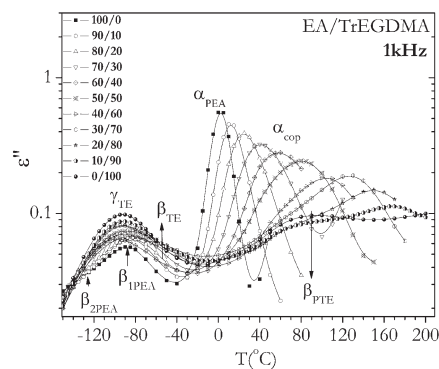


Figure 3. Isochronal plots of the imaginary part of dielectric permittivity at 1 kHz for the overall composition range of EA/TrEGDMA copolymer networks.

Figure 3 shows the dielectric loss against temperature for the overall composition range of EA/TrEGDMA copolymer networks. The evolution of the primary relaxation process (α relaxation) connected with cooperative polymer conformations attracts the main interest in the copolymer networks with varying TrEGDMA content. For the no reticulated PEA, the α_{PEA} process is located at 0 °C. By increasing cross-linker agent content, the α_{cop} relaxation shifts toward higher temperatures. Characteristic is also the significant increase of α_{cop} breadth and decrement of its intensity with the addition of TrEGDMA. On the opposite direction, starting from the net-TrEGDMA (0/100), Figure 3 illustrates the emergence of α_{cop} relaxation process, even for the copolymer network 10/90 approximately at 170 °C, though with quite low strength. By further increase in EA content, α_{cop} relaxation peak shifts toward lower temperatures and increases in magnitude.

The copolymer networks present also several local processes ascribed to both components (Figure 3). The no reticulated PEA presents two relaxation processes in terms of increasing temperature, denoted as $\beta_{1\text{PEA}}$, $\beta_{2\text{PEA}}$ associated with local motions of acrylic branches that are also observed in copolymers with high EA contents ($w_{\text{TE}} < 40$ wt %) at –90 and –120 °C.^{45,46} For TrEGDMA contents $w_{\text{TE}} > 30$ wt %, the γ_{TE} relaxation process is emerged overlapping gradually the PEA secondary processes $\beta_{1\text{PEA}}$, $\beta_{2\text{PEA}}$. The γ_{TE} relaxation process is a local relaxation process attributed to twisting motions of ethylene glycol groups of TrEGDMA (similar to that of poly(ethylene oxide)) lying at –90 °C (at 1 kHz).⁴¹ Interesting enough is the presence of the local secondary relaxation denoted as β_{PTE} lying at 90 °C (1 kHz) which is apparent only for high TrEGDMA contents ($w_{\text{TE}} > 30$ wt %). According to Viciosa et al.,⁴¹ it is attributed to the π -flip motion of acrylic branch around the –C–C– bond that links it to the main chain, coupled to a small rotation of the chain backbone around its local chain axis. The attribution was made based on the similarity of the detected process with β relaxation found in poly(*n*-alkyl methacrylates) which origin is given in refs 47 and 48. For the EA/TrEGDMA copolymer networks 40/60 and 30/70, β_{PTE} appears in the low-temperature side of the α_{cop} process, while for the copolymer networks 20/80, 10/90, and 0/100 it is well discerned. The presence of β_{PTE} is linked with the polymerization of TrEGDMA because it is observed by dielectric spectroscopy only during the polymerization of TrEGDMA monomer, so denoted as β_{PTE} .⁴¹ Furthermore, a new secondary relaxation process is present at the high-temperature side of γ_{TE} process designated as β_{TE} . The strength

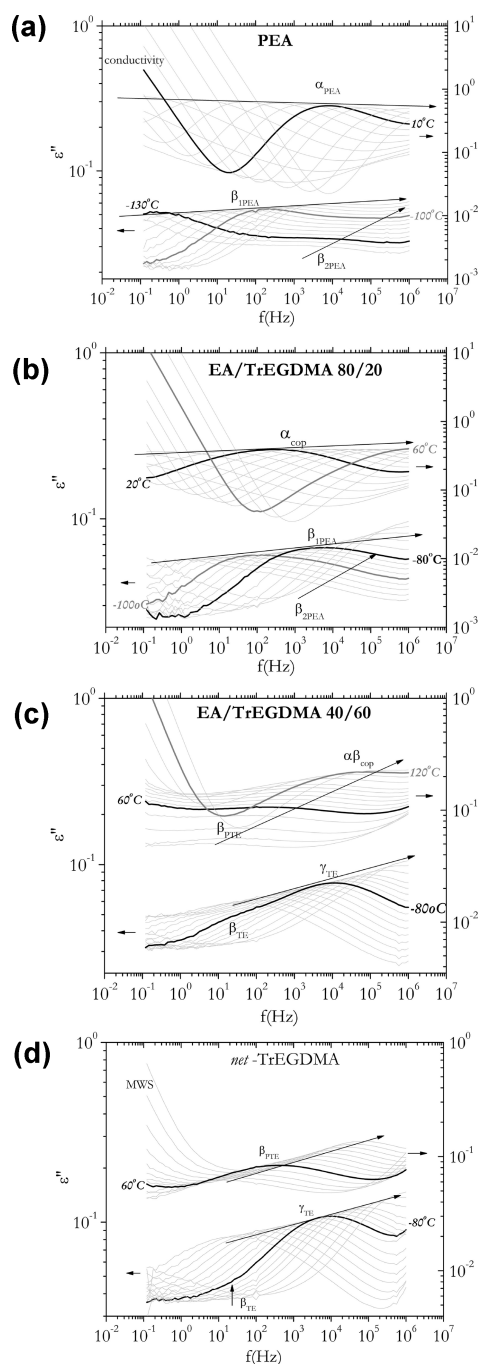


Figure 4. Isothermal plots of the imaginary part of dielectric permittivity against frequency for four representative EA/TrEGDMA compositions: (a) homopolymer PEA, (b) copolymer network 80/20, (c) copolymer network 40/60, and (d) the net-TrEGDMA.

of this process varies not systematically with TrEGDMA content and exists only for high TrEGDMA contents ($w_{TE} > 40$ wt %). Its presence implies the existence of local motions related with unreacted methacrylate double bonds that were trapped during the first stage of polymerization and do not induce postpolymerization because the trapping annihilates their reactivity.^{21,22,32,33,35}

The isotherms of imaginary part of dielectric permittivity against frequency are shown in Figure 4 for the linear PEA, the net-TrEGDMA (PTE), and for two representative copolymer networks EA/TrEGDMA 80/20 and 40/60, respectively, namely

one copolymer network with relatively low amount of TrEGDMA and another one with high amount of TrEGDMA. The no reticulated PEA dielectric response is depicted in Figure 4a revealing the α_{PEA} relaxation process (temperature range -30 to 30 °C) and two secondary relaxations β_{1PEA} and β_{2PEA} (-140 to -80 °C). Within our measuring frequency window, we follow the α_{PEA} process that promptly shifts toward high frequencies with increasing temperature. On the other hand, the net-TrEGDMA is depicted in Figure 4d. Its dielectric response is entirely different compared to linear PEA. Three relaxations are observed in net-TrEGDMA designated as β_{PTE} ($+20$ to $+140$ °C), γ_{TE} (-120 to -30 °C), and β_{TE} at the high-frequency side of γ_{TE} (Figure 4d), while a tremendous MWS process is evident at low frequencies and high temperatures in consistency with TSDC results.

The dielectric results of the two representative copolymer networks are portrayed in Figures 4b,c. Figure 4b portrays the representative dielectric spectra for relatively low contents of the cross-linker agent TrEGDMA, namely for the sample 80/20. We follow the α_{cop} (-5 to 60 °C) that promptly shifts toward high frequencies with increasing temperature obviously appeared at greater temperatures compared to no reticulated PEA (-30 to 30 °C). The secondary relaxations observed for the sample 80/20 are β_{1PEA} and β_{2PEA} (-140 to -80 °C). Similarly, the copolymer networks 90/10 and 70/30 exhibit the same relaxation peaks (results not shown here).

For intermediate and high contents of TrEGDMA ($w_{TE} \geq 40$ wt %), the features of the dielectric spectra are different. In particular, Figure 4c shows a representative dielectric spectrum for the copolymer network 40/60, where it is obvious the presence of the β_{PTE} relaxation well observed above 10 °C within our measuring frequency window. By following β_{PTE} process with increasing temperature, it is evident the slow shift toward higher frequencies. Compared to net-TrEGDMA (Figure 4b) and contrary to that behavior, the β_{PTE} relaxation peak in 40/60 increases in magnitude at temperatures above the respective glass transition temperature, implying that the nature of this process changes within this temperature region (the same is observed also in copolymer networks 60/40, 50/50, 30/70; results not shown here). Noteworthy is the fact that the α_{cop} process is not discerned in dielectric loss isotherms due to the presence of non-dipolar contributions at low frequencies. As concerns the secondary relaxations detected at low temperatures, the local processes γ_{TE} and β_{TE} are apparent. The results have shown that β_{TE} is intensively apparent for copolymer networks with TrEGDMA contents higher than 30 wt %.

In the following, we will focus mainly on α_{cop} relaxation process which is associated with cooperative conformations of polymer segments and the high-temperature β_{PTE} relaxation process. The α_{cop} relaxation peaks were fitted using the Havriliak–Negami model function while for the β_{PTE} relaxation peaks fitting to the one-parameter Cole–Cole model function provided satisfactory results.⁴⁹ Thus, concerning the copolymers with TrEGDMA contents $w_{TE} \leq 30$ wt %, a single HN curve was used to fit the α_{cop} relaxation peak, whereas a single CC curve could be adjusted satisfactorily to the experimental data for higher TrEGDMA contents monitoring the β_{PTE} process. In both cases a conductivity term was also used for the best adjustment at high temperatures:

$$\varepsilon^*(\omega) = \varepsilon_{\infty} + \frac{\Delta\varepsilon}{(1 + (i\omega\tau_{HN})^{\alpha})^{\beta}} - i\left(\frac{\sigma}{\varepsilon_0\omega}\right)^s \quad (1)$$

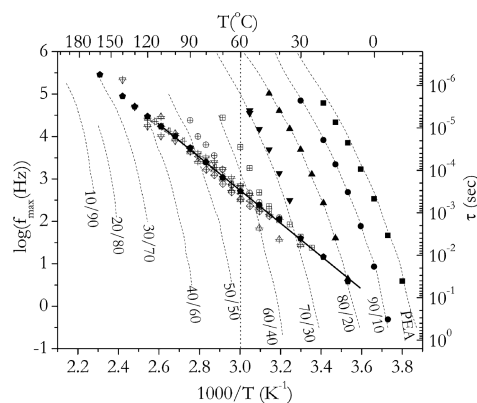


Figure 5. Time scale plot (Arrhenius diagram) involving the temperature dependence of β_{PTE} and α_{cop} relaxation for the overall EA/TrEGDMA composition range [solid symbols: 0/100 (pentagon), 100/0 (square), 90/10 (circle), 80/20 (up triangle), 70/30 (down triangle); crossed-open symbols: 60/40 (square), 50/50 (circle), 40/60 (up triangle), 30/70 (down triangle), 20/80 (rhombus), and 10/90 (left triangle)]. The dashed curves correspond to the α_{cop} experimental data extracted from the respective isochronal plots, while the experimental points are produced by the respective fitting procedure applied to isothermal plots. The solid line represents the trace of β_{PMMA} and β_{PEMA} relaxation processes, as is given in the literature.^{51–53}

where $\Delta\epsilon$ is the relaxation strength, ϵ_{∞} is the limit to high frequencies of the real component of the complex permittivity, ϵ^* , ω is the angular frequency, τ_{HN} is the characteristic relaxation time, α and β are shape parameters, ϵ_0 is the dielectric permittivity of vacuum, σ is the dc conductivity, and s is an exponential ranging $0 \leq s \leq 1$.

The fitting procedure provides the characteristic relaxation time (τ_{HN}) which is related to the characteristic frequency (f_{HN}) through the equation $\tau_{\text{HN}} = 1/(2\pi f_{\text{HN}})$. The peak frequency (f_{max}) is related to the shape parameters α and β and is evaluated through the expression

$$f_{\text{max}} = f_{\text{HN}} \left(\frac{\sin\left(\frac{\alpha\pi}{2 + 2\beta}\right)}{\sin\left(\frac{\alpha\beta\pi}{2 + 2\beta}\right)} \right)^{1/\alpha} \quad (2)$$

Namely for a symmetric relaxation process ($\beta = 1$) we get $f_{\text{max}} = f_{\text{HN}}$.

The temperature dependence of the time scale of the respective relaxation processes obtained from fitting procedure (f_{max}) is depicted in the Arrhenius plot (Figure 5). Temperature dependence of cooperative relaxation processes are well described by the Vogel–Tamman–Fulcher expression:^{50,51}

$$f_{\text{max}} = f_0 e^{-B/(T - T_0)} \quad (3)$$

where f_0 is the pre-exponential factor, B is a phenomenological parameter, and T_0 is the Vogel temperature. The temperature dependence of local relaxation processes is well described by the Arrhenius equation:

$$f_{\text{max}} = f_0 e^{-E_a/k_B T} \quad (4)$$

where f_0 is the pre-exponential factor, E_a is the respective activation energy, and k_B is the Boltzmann constant.

The classification of temperature dependence of α process relaxation times in various glass formers is described by fragility

Table 2. Apparent Activation Energies of the Relaxations β_{PTE} and $\alpha\beta_{\text{cop}}$ as Well as Parameters of the VTF Adjustment and Fragility Regarding the α Relaxation^a

EA/TrEGDMA	$E_a^{\beta_{\text{PTE}}}$ (kJ/mol)	$E_a^{\alpha\beta_{\text{cop}}}$ (kJ/mol)	$\log f_0$	B (K)	T_0 (K)	m
0/100	74.2		14.2			
10/90	73.3		14.6			
20/80	73.1		14.2			
30/70		82.5	15.4			
40/60		85.9	16.0			
50/50	71.9	133.6	14.1			
60/40	79.9	181.0	15.4			
70/30			11.6	1534	237	83
80/20			11.1	1168	234	89
90/10			10.8	1053	227	91
100/0			10.6	959	221	89

^a For the copolymer networks 30/70 and 40/60 a single fit for the overall temperature range was performed, including both the β_{PTE} in the glassy state and $\alpha\beta_{\text{cop}}$ in the rubbery state.

index,⁵² which measures the extent of the deviation from the Arrhenius temperature dependence. It is defined as the slope of relaxation times at glass transition temperature. According to Böhmer et al.⁵³

$$m = 16 + \frac{590}{D} \quad (5)$$

where D is the strength parameter evaluated through VTF expression, namely, through the equation ($B = DT_0$).

Concerning the two components, the temperature dependence of α_{PEA} relaxation process is well described by the VTF expression. The obtained fitting parameters are tabulated in Table 2. On the other side, for net-TrEGDMA the β_{PTE} process shows Arrhenius temperature dependence with activation energy 74.2 kJ/mol. At this point we would like to stress the coincidence in Figure 5 of the position of the β_{PTE} process with the trace of the PMMA and PEMA β process (β_{PMMA} and β_{PEMA} , from the literature^{51–54}) and the respective proximate activation energies of the corresponding processes (75.2 kJ/mol for PMMA and 72.3 kJ/mol for PEMA).^{54–57} This result is not completely unexpected since upon polymerization of TrEGDMA, the covalent bonds establish adjacent to the esteric units in a such way that the main chain of the polymer under formation is similar to a poly(methyl methacrylate), with now the ethylene glycol groups connecting different main chains.⁴¹

For the copolymer networks with low TrEGDMA content ($w_{\text{TE}} \leq 30$ wt %) the temperature dependence of α_{cop} relaxation process follows VTF law and the process is retarded with increasing TrEGDMA content. The VTF parameters obtained by fitting VTF eq 3 to the experimental data are given in Table 2. It is worth noticing that the respective position of α_{cop} relaxation peak obtained by the isochronal data (the respective dashed curves in Figure 5) almost coincides with the peak positions in the spectra recorded isothermally. The fragility index of α_{cop} process relaxation times was evaluated, in this composition range, by means of expression 5. To ensure comparable results, the fitting to VTF expression was carried out by locking the parameter $\log f_0 = 13$.⁵⁸ The results indicate a fragility index that is almost constant in this composition range, taking into

consideration uncertainties in the evaluated value due to the short temperature–frequency range of relaxation times (Table 2). This opposes results in polymer networks with different cross-linking density indicating higher fragility index the higher the cross-linker density.^{8,9,15,19} This behavior has been explained by invoking the increase of interchain interactions and subsequently of the cooperativity due to induced chemical cross-link junctions. On the other hand, Fitz et al.¹³ found that the increase of cross-links in PMPS does not affect the fragility index, meaning that the correlation length of cooperativity is lower than the length between the chemical cross-link junctions.

Interesting enough is the dielectric map for TrEGDMA contents $w_{TE} \geq 40$ wt %. As already mentioned, the detected relaxation processes are mainly ascribed to TrEGDMA moieties. For 10/90 and 20/80 copolymer network the fitting procedure was performed by following the β_{PTE} relaxation processes and their positions coincide with that of net-TrEGDMA presenting contiguous activation energies (Table 2). For 30/70 and 40/60 the fitting of β_{PTE} is more difficult due to reduced intensity and due to high conductivity contributions at low frequencies. Nevertheless, the fitting procedure reveal that the β_{PTE} time scale has not been altered (same positions of peak frequencies in Figure 5 with that for copolymers with higher TrEGDMA contents), indicating that both the dynamics and the local character of β_{PTE} process are not dependent on the TrEGDMA content. For intermediate content of TrEGDMA, namely for the copolymer networks 50/50 and 60/40, the fitting procedure on β_{PTE} relaxation peak reveals a crossover region, where the traces of $\beta_{PTE}f_{max}$ deviate from its initial Arrhenius line toward higher frequencies by increasing temperature exhibiting a new trend with higher activation energy (Figure 5 and Table 2). This deviation occurs ~ 20 deg above their respective calorimetric glass transition. The temperature dependence of f_{max} after the deviation is not clear whether obeys VTF or Arrhenius behavior due to limited experimental data. In any case it is certain that the activation energy for the relaxation process significantly increases. The effect is more pronounced for 60/40 copolymer.

Despite the fact that the isothermal curves of the imaginary part of dielectric permittivity do not indicate a discerned α_{cop} process, the isochronal plots provide a well-defined corresponding peak. Thus, as a comparison with the fitting results on isothermal data, we read the α_{cop} peak temperature in a sequence of isochronal plots for several frequencies and compositions. The results are shown in the Arrhenius plot (Figure 5) in the form of dashed lines for the sake of clarity. The results show the temperature dependence of α_{cop} for a wide range of copolymer compositions (Figure 5). Noteworthy is the fact that by adding EA moieties the α_{cop} becomes faster and merges with β_{PTE} relaxation process presenting a single peak at high frequencies. This merging is more pronounced for the copolymer networks 50/50 and 60/40 and is the reason for the deviation of $\beta_{PTE}f_{max}$ toward $\alpha\beta_{cop}$ (change in activation energy). For samples 40/60 and 30/70 the merging occurs at higher frequencies and temperatures, while for 20/80 and 10/90 it seems to be out of the measured temperature/frequency range. In conclusion, the increase of EA content shifts the merging region toward lower temperatures. This behavior seems to be similar to the shift in the merging region which was observed in poly(*n*-butyl methacrylate-*stat*-styrene) random copolymers by Kahle et al., where the induction of styrene content shifts this crossover region toward higher temperatures.⁵⁹

For the copolymer networks 50/50 and 60/40 the merging between the α_{cop} relaxation and β_{PTE} occurs at temperatures that

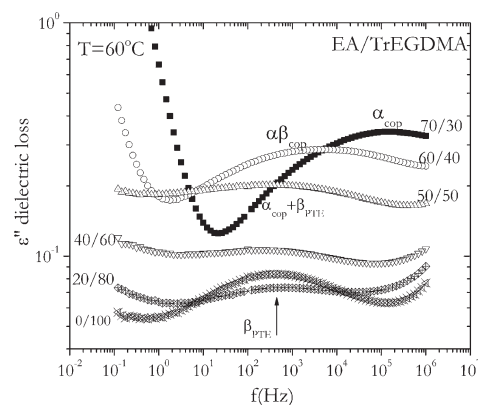


Figure 6. Imaginary part of the dielectric permittivity against frequency for several EA/TrEGDMA composition captured at 60 °C.

are inside the measured frequency window. Figure 6 depicts this merging at different stages of coexistence of α_{cop} and β_{PTE} processes, and this was achieved by changing the EA content. The specific temperature at 60 °C (indicated by the vertical dotted line in Figure 5) was selected as more appropriate because at this temperature all stages of merging are within our measuring frequency window. For the copolymer network 20/80 it is apparent the β_{PTE} process at 400 Hz as in the neat net-TrEGDMA. For the 40/60 the intensity of β_{PTE} is increased, probably due to gradual overlapping with the high frequency tail of α_{cop} process. For the 50/50 and at this temperature the system exhibits an intensive, broad, and complicated relaxation process. According to isochronal results of imaginary part of dielectric permittivity, there is a strong overlapping between α_{cop} and β_{PTE} process (though the individual processes are not resolved in isothermal measurements). Taking also into consideration the position of β_{PTE} and α_{cop} relaxation processes at 60 °C in the Arrhenius plot of Figure 5, the recorded isotherms actually are the superposition of the relaxations α_{cop} and β_{PTE} , indicating that this window illustrates the (β) regime of crossover region according to Garwe et al. for the sample 50/50.⁵⁵ So the relaxation is denoted as $\alpha_{cop} + \beta_{PTE}$. For the 60/40 the relaxation is characterized as $\alpha\beta_{cop}$, and the system might be at the respective (α) regime according to the scheme of merging proposed in ref 52. For the copolymer network 70/30 the relaxation process at high frequencies represents the individual α_{cop} relaxation.

The presence of the merging region (b) and the subsequent single $\alpha\beta_{cop}$ relaxation (region (a)), for the copolymer networks 30/70, 40/60, 50/50, and 60/40, is also verified from the temperature dependence of the dielectric strength of β_{PTE} relaxation process (Figure 7a). By following the dielectric strength of β_{PTE} relaxation process with increasing temperature, for the samples 60/40 and 50/50 it is evident that the dielectric strength reaches a maximum value at approximately 50 and 70 °C, respectively (vertical dotted lines in Figure 7). According to Donth and experimental findings in similar studies, this maximum indicates the crossover from the merging region, where both α and β relaxations are overlapped to the single $\alpha\beta$ process.^{59,60} The dielectric strength of β process increases rapidly until a maximum value and then decreases (scenario I according to Donth classification⁶⁰). The starting point of decreasing marks the onset of a single $\alpha\beta$ process whose dielectric strength decreases with temperature.^{59,60} It is noteworthy that the peak temperature of the respective dielectric strength coincides with the temperature where in

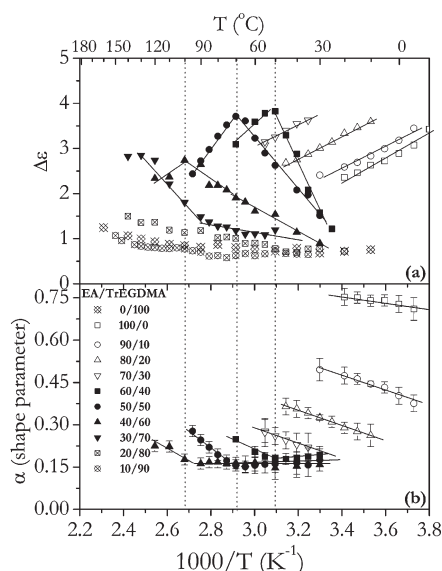


Figure 7. (a) Dielectric strength and (b) α broadening shape parameter, regarding the α_{cop} and β_{PTE} relaxation processes against the reciprocal temperature (bottom axis) and temperature (top axis) for the overall EA/TrEGDMA composition range.

Arrhenius plots of Figure 6 the peak frequency of the β_{PTE} process deviates from the low temperature linear trace, as described previously. The onset of $\alpha\beta_{\text{cop}}$ process presents higher activation energy and implies the cooperative nature of this process.^{61,62} For the samples 40/60 and 30/70 the measuring range marginally records this crossover at 100 and 130 °C, respectively, while for the samples 20/80, 10/90, and net-TrEGDMA the β_{PTE} is still in the glassy state and its dielectric strength increases slightly with temperature.

For the low contents of TrEGDMA ($w_{\text{TE}} \leq 30$ wt %), we monitor the dielectric strength of the α_{cop} relaxation process. Figure 7a shows the decrease of α_{cop} relaxation dielectric strength with increasing temperature as it is anticipated for relaxation process of cooperative character.⁶⁰ Interesting enough is the comparable (or even higher) values of α_{cop} dielectric strength for the samples 90/10, 80/20, and 70/30 as compared to the no reticulated PEA. This specific result seems to be not in consistency with the previous findings of increase of glass transition temperature and decrease of heat capacity increment with increasing TrEGDMA content. However, we have to take into consideration that the dielectric strength $\Delta\epsilon$ is very sensitive to the mean dipole moment μ_0 of the probed segments ($\Delta\epsilon \propto \mu_0^2/T$). TrEGDMA moieties possess relatively strong dipole moment rendering this substitute fairly dielectrically active. This is also reflected in the enhanced dielectric strength of the secondary relaxation processes γ and β as compared to that of EA local relaxation process (Figures 3 and 4). Thus, the impending reduction of dielectric strength due to cross-linking seems to be compensated by the increase of the mean dipole moment introduced by the collaborated TrEGDMA moieties in the segmental motions.

The breath of the recorded relaxation peaks can be quantified by the use of the respective α shape parameter determined by the procedure of fitting the HN function to the α_{cop} relaxation data and the CC function to the β_{PTE} relaxation data. In Figure 7a we present the obtained values of those shape parameters. As

concerns the α_{cop} process, we observe the significant decrement in α parameter, which indicates the increase of α_{cop} breadth with increasing cross-linker content (for $w_{\text{TE}} < 40\%$). This is in consistency with results reported for several polymer networks.^{8–12} On the other hand, quite interesting is the quantification of the shape breadth for β_{PTE} . Specifically, for the copolymer networks 60/40, 50/50, and 40/60 we observe that for temperatures higher than a specific temperature (50, 70, and 100 °C, respectively), the relaxation process becomes progressively narrower with increasing temperature (shape parameter increases), while at lower temperatures the shape remains almost constant. Interestingly, these specific temperatures coincide with the respective temperatures at which the maximum in dielectric strength occurs, as is indicated by the vertical dotted lines in Figure 7. In addition, these characteristic temperatures are the same with those where the traces of peak frequencies deviate from the linear temperature dependence in the Arrhenius plots of Figure 5 for the respective copolymer networks.

DISCUSSION

EA/TrEGDMA Molecular Dynamics: Critical Cross-Linker Agent Content. In order to understand the molecular dynamics of the EA/TrEGDMA copolymer series, the study of the respective homopolymers was essential. Our results obtained by means of TSDC and DRS techniques show that the homopolymers PEA and net-TrEGDMA comprise two entirely different systems. The no reticulated PEA dielectric response manifests a primary relaxation process (α_{PEA}) and the characteristic secondary processes ($\beta_{1\text{PEA}}$ and $\beta_{2\text{PEA}}$) as a typical poly(*n*-alkyl acrylate).^{45,46,54} On the other side, net-TrEGDMA dielectric behavior is characterized by the absence of a cooperative primary relaxation process and by the dominant presence of a MWS peak. The relaxation processes that are present in net-TrEGDMA are the local relaxation processes β_{PTE} , γ_{TE} , and β_{TE} . The respective DSC thermogram does not indicate a distinct glass transition in consistency with dielectric results. All these results lead to the conclusion that net-TrEGDMA is a highly dense polymer network totally different than linear no reticulated PEA. In such a dense polymer network, segmental motions are entirely suppressed, and this behavior is well-established for the reticulated dimethacrylates.^{11,21,33,35}

The combination of EA and TrEGDMA components forms a copolymer network. The dielectric characteristics of these copolymer networks reveal the component that dictates the dynamics of the respective copolymer. The study of the respective primary and secondary relaxation processes suggests the existence of a critical cross-linker content. This critical content range describes the crossover from the EA dominated dynamics to that of the dimethacrylate (cross-linker) one and has been found to be between 30 and 40 wt % of TrEGDMA. Below this critical content region, the spatial morphology of this network, and consequently the molecular dynamics, may be guided by EA component, presenting a single cooperative process α_{cop} relaxation and the domination of EA secondary processes $\beta_{1\text{PEA}}$ and $\beta_{2\text{PEA}}$ at low temperatures. Above this critical content region, the copolymer networks present the dynamical characteristics of the dimethacrylates with the presence of high degree of heterogeneity the more TrEGDMA content. The α_{cop} relaxation is masked by MWS polarization processes and conductivity effects (α_{cop} relaxation is apparent only in isochronal plots at relatively high frequencies), and TrEGDMA originated secondary processes dominate at high (β_{PTE}) and low temperatures (β_{TE} and γ_{TE}).

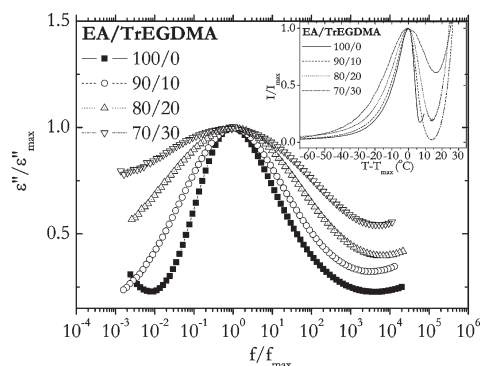


Figure 8. Normalized plots of low TrEGDMA content copolymer networks captured around at 100 Hz. Inset: normalized plots of low TrEGDMA content copolymer networks within the α_{cop} relaxation region recorded by the TSDC technique.

The topology of the copolymers as well as the high degree of spatial heterogeneity for high TrEGDMA contents is explained taking into consideration the different reactivity of the two components during the radical copolymerization. The key factor is the higher reactivity for TrEGDMA radicals compared to EA radicals.²³ It is evident that once the amount of TrEGDMA is above 30 wt %, it has the tendency to form dense cross-linked regions (microgels), which contains exclusively TrEGDMA moieties.^{22,23,33,39} This indicates that a significant amount of TrEGDMA is not incorporated with EA forming thus its own phase and inducing with this manner spatial heterogeneity. In copolymers with high content of TrEGDMA the induction of EA moieties facilitates the creation of islands with higher mobility compared to that of microgel regions. These islands are loosely cross-linked regions, located around the microgel regions.^{33,39} Subsequently, it is anticipated that the EA moieties are copolymerized with TrEGDMA moieties in these regions, while the rigid microgels are regions consisted of exclusively dimethacrylate (TrEGDMA) component. Nevertheless, no dynamic heterogeneity has been detected by dielectric techniques and the DSC technique because the highly cross-linked domains are extremely constrained to produce segmental motions. On the other hand, for low TrEGDMA contents, it is anticipated that TrEGDMA moieties react with EA radicals until their consumption. In this case, the presence of highly cross-linked regions is not prominent.

For low TrEGDMA contents ($w_{\text{TE}} < 40$ wt %), the EA/TrEGDMA system presents a single segmental process (α_{cop}) that becomes slower and broader compared to no reticulated PEA (α_{PEA}). In Figure 8 we show the scaled diagrams corresponding to the segmental relaxation process as is recorded by DRS and TSDC (inset in Figure 8) measurements. We observe that both techniques show the broadening of the relaxation process, indicating the increased heterogeneity caused by the random distribution of cross-linking junctions. The quantification of this broadening is achieved with the use of the shape parameters shown in Figure 7b, where the HN shape parameter (α) drops from the value of 0.75, for the no reticulated PEA, somewhat toward 0.25 for the copolymer network 70/30. Characteristic of this broadening is that the α_{cop} process tends to become symmetrical (the asymmetry shape parameter β of HN distribution tends to $\beta = 1$). These findings are in consistency with results that have been obtained for several polymer networks by increasing

the cross-linking density.^{9,10,12} The aforementioned results show that the dynamics in EA/TrEGDMA copolymer networks rich in EA is governed by EA moieties, though affected by the addition of TrEGDMA moieties that simultaneously reticulates EA and induces heterogeneities in cross-linking distribution. The retardation of α_{cop} dynamics and the broadening of α_{cop} process proclaim that the introduction of TrEGDMA moieties produces a randomly cross-linked polymer exhibiting a distribution of mobilities and subsequently a distribution of relaxation times. On the other hand, despite the induction of steric hindrances from the TrEGDMA moieties, it is evident that they take part in cooperative conformations (α_{cop} relaxation) as is suggested by the comparable dielectric strengths among the no reticulated PEA and the copolymer networks 90/10, 80/20, and 70/30 (Figure 7a).

As already mentioned, for high TrEGDMA contents ($w_{\text{TE}} \geq 40$ wt %) the EA/TrEGDMA copolymer networks exhibit dynamic features originated from the TrEGDMA component. Moreover, the copolymer networks have a highly heterogeneous structure, characterized by the presence of TrEGDMA composed microgels. Interesting enough is the fact that the addition of EA activates segmental motions (α_{cop} relaxation process, not present in net-TrEGDMA) even for the highly dense copolymer network 10/90, though detected only through the isochronal plots of the imaginary part of dielectric permittivity at high frequencies and temperatures. We suppose that the EA moieties are copolymerized with TrEGDMA in loosely cross-linked regions, facilitating in this manner the cooperative conformations which lead to the α_{cop} process. By increase of EA content more domains within the copolymer matrix are involved in these cooperative motions coexisting with the TrEGDMA rigid domains. The increase of EA moieties enhances and accelerates this segmental process which shifts to lower temperatures (Figures 3 and 5). This result indicates that despite the fact that dimethacrylate features dominates, the EA units operate as softener in the highly densified cross-linked EA/TrEGDMA heterogeneous copolymer networks.

α – β Merging Region in EA/TrEGDMA Copolymer Networks. Another characteristic feature of EA/TrEGDMA copolymer networks dynamics with TrEGDMA contents $w_{\text{TE}} \geq 40$ wt % is the merging of segmental relaxation process and β_{PTE} relaxation process in a way similar to that in poly(*n*-alkyl methacrylates). By following the β_{PTE} relaxation process, starting from the net-TrEGDMA, it is obvious that the addition of EA moieties does not change the time scale of the process (Figure 5). In this process contribute molecular motions activated in both domains, rigid TrEGDMA domains (microgels) and loosely cross-linked regions softened by EA moieties. On the other hand, within the loosely cross-linked regions a faster cooperative process is activated, increasing in magnitude with increasing EA content. As a consequence, we observe that the addition of EA moieties affects significantly the temperature dependence of β_{PTE} dielectric strength: in a specific temperature interval it increases rapidly with increasing temperature, and the more EA content the lower the temperature where this increase is first observed (Figure 7a). Comparisons with dielectric results of PMMA and PEMA, performed in our laboratory and appearing in the literature,^{54–56} show that the β_{PTE} process is characterized by the same activation energy and time scale with the β process in the glassy state for PMMA and PEMA (Figure 5). Furthermore, by performing analysis in dielectric data obtained by DRS measurements, significant evidence was found support the merging of β_{PTE} and α_{cop} toward $\alpha\beta_{\text{cop}}$ single process. Indeed, the temperature

dependence of the peak frequency (Figure 5), of the dielectric strength of β_{PTE} process, and of the shape parameter of that process (Figure 7) exhibits features similar to that presented in the merging region of α and β relaxation processes toward the $\alpha\beta$ process in poly(*n*-alkyl methacrylates).^{55,59,63–65} These features are more pronounced in copolymer networks 60/40, 50/50, and 40/60, where the amount of EA is adequate enough to facilitate segmental motions within a dimethacrylate dominated network. Moreover, our results allow for monitoring the merging of α_{cop} relaxation with the local process β_{PTE} toward $\alpha\beta_{\text{cop}}$ process in copolymer networks with varying TrEGDMA content (for $w_{\text{TE}} \geq 40$ wt %). With decreasing TrEGDMA content/increasing EA content the α_{cop} process shifts toward higher frequencies/lower temperatures (becomes faster) (Figures 5 and 6). Thus, at a certain range of compositions (30–60 wt % of EA) this merging occurs at the frequency/temperature window of our experimental setup, and then it is accordingly recorded. Thereby, the merging region is controlled by the presence of EA moieties that softens the loosely cross-linked regions and subsequently shift the merging region toward lower temperatures (Figures 5–7).

A similar shift of the merging region has been reported in statistical copolymer networks and polymer blends with the one component being a poly(alkyl methacrylate).^{59,66,67} The shift of the merging region has been also observed in poly(*n*-alkyl methacrylates) by changing the length of the side chain.^{54,55} In those systems the increase in the length of the methacrylate branch causes the shift of the α process toward lower temperatures, and subsequently the merging region of α and β processes migrates toward lower frequencies and temperatures. In both cases the α relaxation process and subsequently the dynamic glass transition change by changing either the structure or the steric hindrances that affect the specific merging region where the local process and a cooperative one are coupled. Ngai et al. have studied thoroughly the effect of molecular structure, tacticity, molecular weight, copolymerization, and nanoconfinement to this coupling.⁶³

According to the scheme proposed by Garwe et al.,⁵⁵ the merging (splitting region) is consisted of three regimes. The (c) regime corresponds to glassy state where only the β relaxation process is activated, the (b) regime corresponds to the temperature range above the glass transition where α and β processes co-exist, and the (a) regime where the single process $\alpha\beta$ is present. Garwe and co-workers have also suggested that the $\alpha\beta$ single process is locally cooperative.⁵⁵ In the present system the merging of α_{cop} and β_{PTE} leading to the single $\alpha\beta_{\text{cop}}$ was detected only for copolymer networks 60/40, 50/50, and marginally for 40/60. Therefore, at least for that copolymers, and in analogy with the merging scheme proposed for the methacrylates, our results suggest that the β_{PTE} mechanism changes from a local process below glass transition temperature to a process with cooperative character above T_g .

For the same copolymers it is noteworthy the absence of specific change from the (c) regime to (b) regime in the corresponding Arrhenius plots in Figure 5. This implies that the dynamical characteristics of the β_{PTE} process do not change in the temperature region around the calorimetric T_g . For our strongly spatially heterogeneous systems this result might suggest that the cooperative motions detected as segmental mobility can be activated through the EA moieties in isolated loosely cross-linked regions within the dense copolymer network (“islands of mobility”). The local β_{PTE} process originated in molecular motions within the rigid network of TrEGDMA moieties is decoupled from

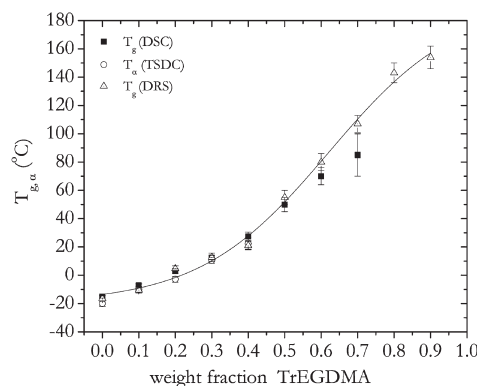


Figure 9. Dynamic (T_{α} and $T_{g,\text{DRS}}$) and thermal glass transition temperature dependence with TrEGDMA fraction. The solid curve is guide for the eyes.

the segmental motions. By increasing temperature the locally cooperative motions within the loosely cross-linked regions dominate and then only the one single relaxation process $\alpha\beta_{\text{cop}}$ survives (regime (c) in the Arrhenius plots). By decreasing EA content, the number of the loosely cross-linked regions contributing to the cooperative conformational rearrangements also decreases.

Glass Transition of EA/TrEGDMA Copolymer Networks against TrEGDMA Content. The dependence of glass transition temperature with increasing TrEGDMA content depicts that this dependence is mainly convex–concave (S-shaped) (Figure 9). This directly confirms that the copolymer networks should not be considered as a simple mixture of two components for the whole composition range. Therefore, the copolymer glass transition dependence on TrEGDMA content does not obey the conventional mixing rules, such as Fox empirical expression, which rely on free volume additivity between the two components. Such a behavior is anticipated mainly from two basic reasons. First, the quite different reactivity ratios between the two components that favors phase separation during the radical copolymerization. Second, the one component is multifunctional and therefore able to develop cross-links, and subsequently it induces strong coupling (interaction) between two components.

For TrEGDMA contents $w_{\text{TE}} \leq 30$ wt % the T_g exhibits an almost linear dependence, in agreement with other systems with comparable cross-linker contents (Figure 9).^{14,17} However, by observing the dependence of T_g on the overall composition range, the inhibition of the glass transition temperature increment for $w_{\text{TE}} > 60$ wt % is obvious. At this point, we explain that the dynamic glass transition has been evaluated through DRS data and, specifically, from the α_{cop} traces in Arrhenius plots of Figure 5, as the temperature, at which the mean relaxation time becomes $\langle \tau \rangle = 100$ s. Subsequently, this value signifies the glass transition temperature originated from the loosely cross-linked regions that surround the microgels or microgel agglomerates. Therefore, the glass transition evaluated from DRS measurements for TrEGDMA contents $w_{\text{TE}} \geq 60$ wt % does not correspond to the respective calorimetric T_g of the sample, if we take into consideration that the T_g values estimated from DSC and TSDC techniques respectively are limited to 70 and 40 wt % of TrEGDMA, respectively. Therefore, it is not feasible the description of the composition dependence of T_g for the overall TrEGDMA content range with any of the empirical equations widely used in polymer blends, copolymers, IPNs, etc.

CONCLUSIONS

The molecular dynamics of EA/TrEGDMA copolymer networks in their overall composition range were investigated by means of the dielectric techniques of thermally stimulated depolarization currents (TSDC) and of dielectric relaxation spectroscopy (DRS). Furthermore, differential scanning calorimetry was employed to investigate the glass transition in these series.

The dielectric characteristics of these copolymer networks indicate that there is a critical TrEGDMA composition range between 30 and 40 wt %, which defines the composition ranges where the final dynamical properties are dictated mainly by the one component. Specifically, below 30 wt % of TrEGDMA content, PEA dynamics dictate the overall dynamical behavior, and consequently, the copolymers exhibit a single segmental relaxation process α_{cop} that becomes slower and broader with increasing TrEGDMA content. Characteristic is the comparable dielectric strength with that of the segmental relaxation process in the no reticulated PEA, implying that TrEGDMA moieties take part to segmental motions, despite the introduction of chemical cross-link junctions that lower the heat capacity increment. Moreover, the secondary relaxation processes of PEA, β_{PEA1} and β_{PEA2} , dominate at low temperatures in this content range.

For the copolymer networks with TrEGDMA content $w_{\text{TE}} \geq 40$ wt % the molecular dynamics exhibits salient dielectric features governed by the TrEGDMA component. The main characteristic of copolymer molecular dynamics in this composition region is that the dimethacrylate dynamics resembles that of poly(*n*-alkyl methacrylates) exhibiting a merging regime where the local β_{PTE} relaxation merges with α_{cop} toward the locally cooperative $\alpha\beta_{\text{cop}}$ relaxation process. This merging region shifts toward lower temperatures with increasing EA content and EA moieties act as plasticizers in the dense and heterogeneous TrEGDMA dominated network. Another characteristic feature of the copolymers in this composition range is that the copolymer networks are quite heterogeneous. This is reflected in the broadening of the segmental relaxation process and the presence of MWS non-dipolar polarization process that is coupled with the α_{cop} process at low frequencies. Concerning the segmental relaxation process detected by DRS measurements in this composition range, our results may be interpreted by the assumption that the underlying cooperative molecular motions may be activated in isolated loosely cross-linked regions, where EA moieties facilitate segmental motions. A main consequence of this is the convex–concave dependence of copolymer glass transition with TrEGDMA content and the absence or the very broad glass transition detected by DSC in copolymers reach in cross-linker agent.

AUTHOR INFORMATION

Corresponding Author

*E-mail: astathop@mail.ntua.gr.

ACKNOWLEDGMENT

A.T.S. thanks the Department of Physics, National Technical University of Athens, for the financial support of this work.

REFERENCES

- (1) Peppas, N. A.; Moyniman, H. J.; Peppas, N. A., Eds.; Wiley & Sons: New York, 1987; Vol. 2, p 49.
- (2) Hoffman, A. S. *Adv. Drug Delivery Rev.* **2002**, *54*, 3–12.
- (3) Bland, M. H.; Peppas, N. A. *Biomaterials* **1996**, *17*, 1109–1114.

- (4) Matsuda, T.; Funae, Y.; Yoshida, M.; Yamamoto, T.; Takaya, T. *J. Appl. Polym. Sci.* **1997**, *65*, 2247–2255.
- (5) Asmusen, S.; Arenas, G.; Cook, W. D.; Vallo, C. *Dent. Mater.* **2009**, *25*, 1603–1611.
- (6) Eric Dietz, J.; Peppas, N. A. *Polymer* **1997**, *38*, 3767–3781.
- (7) Mason, P. *Polymer* **1964**, *5*, 625–635.
- (8) Kramarenko, V. Y.; Ezquerro, T. A.; Sics, I.; Balta-Calleja, F. J.; Privalko, V. P. *J. Chem. Phys.* **2000**, *113*, 447–452.
- (9) Roland, C. M. *Macromolecules* **1994**, *27*, 4242–4247.
- (10) Glatz-Reichenbach, J. K. W.; Sorriero, L.; Fitzgerald, J. J. *Macromolecules* **1994**, *27*, 1338–1343.
- (11) Viciosa, M. T.; Rouzé, N.; Dionísio, M.; Gómez Ribelles, J. L. *Eur. Polym. J.* **2007**, *43*, 1516–1529.
- (12) Dueñas, J. M. M.; Mateo, J. M.; Ribelles, J. L. G. *Polym. Eng. Sci.* **2005**, *45*, 1336–1342.
- (13) Fitz, B. D.; Mijovic, J. *Macromolecules* **1999**, *32*, 3518–3527.
- (14) Sasaki, T.; Uchida, T.; Sakurai, K. J. *Polym. Sci., Part B: Polym. Phys.* **2006**, *44*, 1958–1966.
- (15) Alves, N. M.; Gómez Ribelles, J. L.; Mano, J. F. *Polymer* **2005**, *46*, 491–504.
- (16) Gómez Ribelles, J. L.; Meseguer Dueñas, J. M.; Torregrosa Cabanilles, C.; Monleón Pradas, M. J. *Phys.: Condens. Matter* **2003**, *15*, S1149.
- (17) Bicerano, J.; Sammler, R. L.; Carriere, C. J.; Seitz, J. T. *J. Polym. Sci., Part B: Polym. Phys.* **1996**, *34*, 2247–2259.
- (18) Podgórski, M. *J. Appl. Polym. Sci.* **2009**, *112*, 2942–2952.
- (19) Robertson, C. G.; Wang *Macromolecules* **2004**, *37*, 4266–4270.
- (20) Schroeder, M. J.; Roland, C. M. *Macromolecules* **2002**, *35*, 2676–2681.
- (21) Rey, L.; Galy, J.; Sautereau, H. *Macromolecules* **2000**, *33*, 6780–6786.
- (22) Guo, Z.; Sautereau, H.; Kranbuehl, D. E. *Macromolecules* **2005**, *38*, 7992–7999.
- (23) Gao, H.; Miasnikova, A.; Matyjaszewski, K. *Macromolecules* **2008**, *41*, 7843–7849.
- (24) Lindemann, B.; Schröder, U. P.; Oppermann, W. *Macromolecules* **1997**, *30*, 4073–4077.
- (25) Matsuo, E. S.; Orkisz, M.; Sun, S.-T.; Li, Y.; Tanaka, T. *Macromolecules* **1994**, *27*, 6791–6796.
- (26) Norisuye, T.; Tran-Cong-Miyata, Q.; Shibayama, M. *Macromolecules* **2004**, *37*, 2944–2953.
- (27) Gurtovenko, A. A.; Gotlib, Y. Y. *J. Chem. Phys.* **2001**, *115*, 6785–6793.
- (28) Brás, A. R. E.; Viciosa, M. T.; Rodrigues, C. M.; Dias, C. J.; Dionísio, M. *Phys. Rev. E* **2006**, *73*, 061709.
- (29) Anseth, K. S.; Newman, S. M.; Bowman, C. N. *Adv. Polym. Sci.* **1995**, *122*, 177–217.
- (30) Lovell, L. G.; Stansbury, J. W.; Sympes, D. C.; Bowman, C. N. *Macromolecules* **1999**, *32*, 3913–3921.
- (31) Dickens, S. H.; Stansbury, J. W.; Choi, K. M.; Floyd, C. J. E. *Macromolecules* **2003**, *36*, 6043–6053.
- (32) Chiu, Y. Y.; Lee, L. J. *J. Polym. Sci., Part A: Polym. Chem.* **1995**, *33*, 257–267.
- (33) Kannurpatti, A. R.; Anseth, J. W.; Bowman, C. N. *Polymer* **1998**, *39*, 2507–2513.
- (34) Simon, G. P.; Allen, P. E. M.; Williams, D. R. G. *Polymer* **1991**, *32*, 2577–2587.
- (35) Lovell, L. G.; Berchtold, K. A.; Elliott, J. E.; Lu, H.; Bowman, C. N. *Polym. Adv. Technol.* **2001**, *12*, 335–345.
- (36) Naghash, H. J.; Okay, O.; Yagci, Y. *Polymer* **1997**, *38*, 1187–1196.
- (37) Achilias, D. S.; Karabela, M. M.; Sideridou, I. D. *Thermochim. Acta* **2008**, *472*, 74–83.
- (38) Young, J. S.; Kannurpatti, A. R.; Bowman, C. N. *Macromol. Chem. Phys.* **1998**, *199*, 1043–1049.
- (39) Rey, L.; Duchet, J.; Galy, J.; Sautereau, H.; Vouagner, D.; Carion, L. *Polymer* **2002**, *43*, 4375–4384.
- (40) Viciosa, M. T.; Rodrigues, C. M.; Dionísio, M. J. *Non-Cryst. Solids* **2005**, *351*, 14–22.

- (41) Viciosa, M. T.; Brás, A. R.; Gómez Ribelles, J. L.; Dionísio, M. *Eur. Polym. J.* **2008**, *44*, 155–170.
- (42) Vatalis, A. S.; Delides, C. G.; Georgoussis, G.; Kyritsis, A.; Grigorieva, O. P.; Sergeeva, L. M.; Brovko, A. A.; Zimich, O. N.; Shtompel, V. I.; Neagu, E.; Pissis, P. *Thermochim. Acta* **2001**, *371*, 87–93.
- (43) Van Turnhout, J. In *Topics in Applied Physics. Electrets*; Sessler, G. M., Ed.; Springer-Verlag: Berlin, 1980; Vol. 33, pp 81–215.
- (44) Kremer, F.; Schönhals, A. *Broadband Dielectric Spectroscopy*; Springer: Berlin, 2003.
- (45) Gómez Ribelles, J. L.; Meseguer Dueñas, J. M.; Monleón Pradas, M. *J. Appl. Polym. Sci.* **1989**, *38*, 1145–1157.
- (46) Gaborieau, M.; Graf, R.; Kahle, S.; Pakula, T.; Spiess, H. W. *Macromolecules* **2007**, *40*, 6249–6256.
- (47) Kuebler, S. C.; Schaefer, D. J.; Boeffel, C.; Pawelzik, U.; Spiess, H. W. *Macromolecules* **1997**, *30*, 6597–6609.
- (48) Kulik, A. S.; Beckham, H. W.; Schmidt-Rohr, K.; Radloff, D.; Pawelzik, U.; Boeffel, C.; Spiess, H. W. *Macromolecules* **1994**, *27*, 4746–4754.
- (49) Havriliak, S.; Negami, S. *Polymer* **1967**, *8*, 161–210.
- (50) Vogel, H. *Phys. Z.* **1921**, *22*, 645.
- (51) Fulcher, G. S. *J. Am. Chem. Soc.* **1925**, *8*, 789.
- (52) Angell, C. A. *Science* **1995**, *267*, 1924–1935.
- (53) Böhmer, R.; Ngai, K. L.; Angell, C. A.; Plazek, D. J. *J. Chem. Phys.* **1993**, *99*, 4201–4209.
- (54) McCrum, N. G.; Read, B. E.; Williams, G. *Anelastic and Dielectric Effect in Polymer Solids*; Dover Publications: Mineola, NY, 1967.
- (55) Garwe, F.; Schönhals, A.; Lockwenz, H.; Beiner, M.; Schröter, K.; Donth, E. *Macromolecules* **1996**, *29*, 247–253.
- (56) Ishida, Y.; Yamafuji, K. *Kolloid-Z.* **1961**, *2*, 97–117.
- (57) Gómez, D.; Alegría, A.; Arbe, A.; Colmenero, J. *Macromolecules* **2001**, *34*, 503–513.
- (58) Richert, R.; Angell, C. A. *J. Chem. Phys.* **1998**, *108*, 9016–9026.
- (59) Kahle, S.; Korus, J.; Hempel, E.; Unger, R.; Höring, S.; Schröter, K.; Donth, E. *Macromolecules* **1997**, *30*, 7214–7223.
- (60) Donth, E. *The Glass Transition*; Springer-Verlag: Berlin, 2001.
- (61) Espadero Berzosa, A.; Gómez Ribelles, J. L.; Kripotou, S.; Pissis, P. *Macromolecules* **2004**, *37*, 6472–6479.
- (62) Kyritsis, A.; Gómez Ribelles, J. L.; Meseguer Dueñas, J. M.; Soler Campillo, N.; Gallego Ferrer, G.; Monleón Pradas, M. *Macromolecules* **2003**, *37*, 446–452.
- (63) Ngai, K. L.; Gopalakrishnan, T. R.; Beiner, M. *Polymer* **2006**, *47*, 7222–7230.
- (64) Gaborieau, M.; Graf, R.; Spiess, H. W. *Macromol. Chem. Phys.* **2008**, *209*, 2078–2086.
- (65) Mpoukouvalas, K.; Floudas, G.; Williams, G. *Macromolecules* **2009**, *42*, 4690–4700.
- (66) Zhang, S.; Jin, X.; Painter, P. C.; Runt, J. *Macromolecules* **2002**, *35*, 3636–3646.
- (67) Ngai, K. L. *Macromolecules* **1999**, *32*, 7140–7146.